

# Slow Resonance Ratio Control for Vibration Suppression and Disturbance Rejection in Torsional System

Yoichi Hori, member, Hideyuki Sawada and Yeonghan Chun

Department of Electrical Engineering, University of Tokyo,

7-3-1 Hongo, Bunkyo, Tokyo 113-8656, JAPAN

Tel: +81-3812-2111 ext.7680, Fax: +81-3-5800-3865

E-mail: hori@hori.t.u-tokyo.ac.jp

**Abstract** : In the resonance ratio control, which we proposed for vibration suppression and disturbance rejection in torsional system, the estimation speed of the disturbance observer should have been much faster than the resonance frequency of the controlled system. However, too fast disturbance observer sometimes causes implementation problem. In this paper, we give the optimal speed of the disturbance observer and propose a novel technique named "slow resonance ratio control". It does not have any fast part in the controller. It also enables us to design the speed control and the vibration suppression control almost completely independently.

**Keywords** : vibration suppression, torsional system, speed control, robust control, disturbance observer, disturbance rejection, resonance ratio, observer pole design

## I. INTRODUCTION

Vibration suppression and disturbance rejection control in torsional system is an important problem in the future motion control. As the newly required speed response is very close to the primary resonant frequency of such systems, conventional techniques based only on P&I controller is not effective enough. To overcome the problems, various control strategies have been proposed mainly for controlling 2-inertia system, the simplest model of the flexible system.<sup>[1][2][3][7][12][13][14]</sup>

In this paper, we will focus our discussion onto the disturbance observer-based techniques. We proposed "resonance ratio control" several years ago and showed its excellent performance by numerical simulation.<sup>[4][9]</sup> By feeding back the torsional torque estimated by the disturbance observer, the virtual motor inertia moment can be changed to an arbitrarily value. This means that we can change the resonance frequency and then the resonance ratio.

However, the estimation speed of the disturbance observer used in the resonance ratio control was assumed fast enough compared to the resonant frequency of the controlled object.<sup>[9]</sup> Too fast disturbance observer causes implementation problem. We clarified that slower disturbance estimation degrades various control performances.

In this paper, we propose a novel technique, "slow resonance ratio control", whose advantages are

as follows:

- (1) The optimal speed of the disturbance estimation is given by an explicit formula. It is relatively slow in most cases.
- (2) The speed controller can be designed independently from the vibration suppression control.

Finally, we explain the specially designed experimental setup using two motors and adjustable inertia moments connected by a flexible shaft. We can adjust not only the inertia moments and the stiffness of the shaft but also the backlash and friction. We confirm the effectiveness of the proposed method by experiments.

## II. STEEL ROLLING MILL AND 2-INERTIA MODEL

Fig.1 illustrates the typical configuration of steel rolling mill system. This system is basically a distributed parameter system. By using the modal analysis, it can be modeled as a system having several inertia moments and springs.<sup>[12]</sup> For example, 12 inertia moments are used for simulation but it is too complicated for controller design. 2-inertia system given by Fig.2 is its simplest model. Fig.3 gives its block diagram representation.

In Fig.2, we assume

$$J_{M0} + J_L = 1, \quad K_s = 1 \quad (1), (2)$$

for comparative analysis and controller design. These equations mean that the total inertia moment of the motor and the load, and the spring coefficient are fixed to 1, respectively. Various 2-inertia systems with different inertia ratios will be investigated under these relations.

As frictional effect is usually very small in most industrial systems, by putting  $B_M = B_L = 0$  in Figs.2 and 3, the transfer function from  $T_M$  to  $\omega_M$ , can be approximated by

$$G_{11}(s) = \frac{1}{s} \frac{J_L s^2 + K_s}{J_{M0} J_L s^2 + K_s (J_{M0} + J_L)} = \frac{1}{J_{M0} s} \frac{s^2 + \omega_a^2}{s^2 + \omega_{r0}^2} \quad (3)$$

This transfer function, the most important one for the closed loop characteristics design, has two particular frequency points: the resonant and anti-resonant frequencies given by

$$\omega_{r0} = \sqrt{\frac{K_s}{J_L} \left( 1 + \frac{J_L}{J_{M0}} \right)} \quad (4)$$

$$\omega_a = \sqrt{\frac{K_s}{J_L}} \quad (5)$$

where  $R_0$  is the inertia ratio of the original system given by  $R_0 = J_L / J_{M0}$ . At these frequencies, phase characteristics change drastically, too.

### III. SLOW RESONANCE RATIO CONTROL AND ITS DESIGN METHOD

Fig.4 depicts our new technique: "slow resonance ratio control". Using this configuration, we will explain its idea.

#### A. Ideal Fast Resonance Ratio Control [9][11]

When we put  $T_q=0$  in Fig.4, it gives the ideal "resonance ratio control" based on the fast disturbance observer. In usual disturbance observer applications, 100% of the estimated disturbance is fed back to the motor torque, but in this case,  $1-K$  of the estimated disturbance is fed back. By doing this, we can change the virtual motor inertia moment to any value as

$$J_M = J_{M0}/K \quad (6)$$

The inertia ratio can be changed to

$$R = \frac{J_L}{J_M} = \frac{J_L}{J_{M0}/K} = KR_0 \quad (7)$$

The resonant frequency is then changed to

$$\omega_r = \sqrt{\frac{K_s}{J_L} \left(1 + \frac{J_L}{J_M}\right)} \quad (8)$$

The anti-resonant frequency does not change. In the resonance ratio control, by setting the new resonance ratio  $H=\omega_r/\omega_a$  to be  $2 \sim \sqrt{5}$ , effective vibration suppression is achieved.<sup>[4][9][11]</sup> However, the estimation speed of the disturbance observer can not be infinite in actual systems. From some simulations, it is known that the estimation should be performed much faster than the resonant frequency of the controlled object.

#### B. Slow Resonance Ratio Control

When the estimation speed of the observer is finite, i.e.,  $T_q > 0$ , the ideal resonance ratio control becomes impossible. Generally by using  $Q(s)$  as the low-pass filter part:  $1/(T_q s + 1)$  in Fig.4, the following two important transfer functions can be obtained.

$$\frac{\omega_M}{T_M'} = \frac{1+R}{s} \frac{s^2 + \omega_a^2}{s^2 + \{1 + \{1 - Q(s)\}R_0 + Q(s)R\}\omega_a^2} \quad (9)$$

$$\frac{\omega_L}{T_M'} = \frac{1+R}{s} \frac{\omega_a^2}{s^2 + \{1 + \{1 - Q(s)\}R_0 + Q(s)R\}\omega_a^2} \quad (10)$$

We pay more attention to  $\omega_L/T_M'$ . Its characteristics are as follows.

When the observer is very fast, i.e.,  $T_q=0$  if  $Q(s)=1/(T_q s+1)$ , by putting  $Q(s) = 1$ , eq.(11) is obtained.

$$\frac{\omega_L}{T_M'} = \frac{1+R}{s} \frac{\omega_a^2}{s^2+(1+R)\omega_a^2} = \frac{1}{s} \frac{\omega_r^2}{s^2+\omega_r^2} \quad (11)$$

When the observer is very slow, i.e.,  $T_q = \infty$  if  $Q(s)=1/(T_q s+1)$ , by putting  $Q(s) = 0$ , eq.(12) is obtained.

$$\frac{\omega_L}{T_M'} = \frac{1+R}{s} \frac{\omega_a^2}{s^2+(1+R_0)\omega_a^2} = \frac{1}{s} \frac{\omega_r^2}{s^2+\omega_{r0}^2} \quad (12)$$

These two curves have the intersection point at

$$\omega_0 = \sqrt{1 + \frac{R+R_0}{2}} \omega_a \quad (13)$$

and the amplitude there is given by

$$\frac{\omega_L}{T_M'} = \frac{1+R}{\omega_0} \frac{2}{R-R_0} \quad (14)$$

Interestingly, all curves having any  $T_q$  pass this point. Hence, if  $T_q$  is selected so that this point is the local maximum, vibration suppression can be realized most effectively. Such  $T_q$  is given by

$$T_q = \sqrt{\frac{1 + \frac{R+3R_0}{4}}{\left(1 + \frac{3R+R_0}{4}\right)\left(1 + \frac{R+R_0}{2}\right)}} \frac{1}{\omega_a} \quad (15)$$

This is the optimal estimation speed (the optimal time constant) of the disturbance observer when we use the first order observer.

For reference, the optimal estimation speed given by Iwata in Umida's slow disturbance observer is given by<sup>[5][6]</sup>

$$T_q = \sqrt{1 + \frac{R_0}{2}} \frac{1}{\omega_a} \quad (16)$$

This value is close to one when we put  $R=0$  in eq.(15). In other word, Umida's slow disturbance observer is the special case putting  $R=0$  in the slow resonance ratio control.

### C. Design of $K$

$K$  is the ratio of  $R$  (the new inertia ratio that the resonance ratio control aims to realize) to  $R_0$  (the original inertia ratio), i.e.,  $R=KR_0$ .  $\omega_a$  is also the function of  $R_0$ . When  $R_0$  is given as a parameter

of the original system, from eqs.(14) and (15), the optimal estimation speed  $T_q$  and the peak amplitude at  $\omega_0$  are the functions of only  $K$ .

Fig.5 draws the peak amplitude at  $\omega_0$  as the function of  $K$ . The peak at  $\omega_0$  decreases when  $K$  increases. On the other hand, from Fig.6, we can see that  $\omega_q(=1/T_q)$  becomes bigger when  $K$  increases, which means that faster estimation is required. It must cause implementation problem. Hence we need a compromise.

From Figs. 5 and 6, if we select  $K=5 \sim 10$ , the peak is relatively small while keeping  $\omega_q$  not so big for a wide range of  $R_0$ . For smaller  $K$ ,  $\omega_q$  becomes much smaller, which reduces implementation problem, because the controller has no fast parts.

On the contrary, we can consider the method to optimize  $K$  by evaluating  $|\omega_L/T_m'|$  for a given  $T_q$  and  $R_0$ . These three parameters  $K$ ,  $T_q$  and  $R_0$  have close inter-relation. It is also possible to know the optimal  $K$  from Fig.6 but we did not give its clear formula. In most industrial applications,  $T_q$  is not chosen to be the possible smallest value. Its lower limit was determined by realistic experimental factors like sampling period, noise suppression ability and so on. It may vary according to many factors, e.g., inertia ratio, P&I controller parameters, backlash, and so on. In other word, it is usually difficult to determine the minimum value of  $T_q$  beforehand. This is the reason why we did not determine  $T_q$  first.

#### D. Design of the Speed Controller

In eqs.(9) and (10),  $\omega_L/T_m'$  converges to  $1/s$  when  $s \rightarrow 0$ , because we designed so as to keep their DC gains to be the same value regardless of  $R_0$ . It means that, in all cases with any  $R_0$ , the 2-inertia system can be seen 1-inertia system having  $J_{M0}+J_L=1$  as the total inertia moment.

It is very convenient if we can use the fixed coefficient P&I speed controller designed for 1-inertia system. Here, we put

$$K_p = \frac{1}{T_\omega}, \quad K_i = \frac{K_p}{2.5 T_\omega} \quad (17), (18)$$

$T_\omega$  is the specified response time of speed control. Here, we put  $T_\omega=1/\omega_a$  hoping to realize the command response as fast as the anti-resonant frequency. Eq.(18) means that we selected the integral time constant to be 2.5 times of the speed control response. In simulation, two-degree-of-freedom P&I controller is used to reduce the overshoot in command response. It can be realized simply by putting  $b=0.5$  in Fig.4.

#### E. Summary of the Design Procedure

We summarize the design procedure of "slow resonance ratio control" proposed above.

- (1) Put  $K=5 \sim 10$ , i.e.,  $R=5R_0 \sim 10R_0$ .
- (2) Put the disturbance observer's estimation speed by eq.(15).
- (3) Design the speed controller by eqs.(17) and (18).
- (4) If the designed  $T_q$  is proved too small by experiment, back to (1) and chose smaller  $K$ .

#### IV. SIMULATION RESULTS OF THE SLOW RESONANCE RATIO CONTROL

Fig.7 shows one example of the time response simulation of "slow resonance ratio control" At  $t=5$ ,  $\omega^*=1$  is given as the speed reference to observe its command response characteristics. At  $t=25$ , step disturbance of  $T_L=-0.5$  is given to see the disturbance response.

In this simulation, we made the system parameters to include 10~20% errors, backlash ( $\pm 0.01$ ), and torque limiter ( $\pm 1.2$ ). We can know that the performances of the proposed method are same or superior to other methods proposed until now, e.g., the fast resonance ratio control, the optimal PID control, and even the state feedback control.<sup>[10][11][15]</sup>

The speed controller is designed for 1-inertia system without any consideration on vibration suppression. Such an independent design has a great advantage in actual industrial application systems.

#### V. EXPERIMENTAL RESULTS OF DISTURBANCE OBSERVER BASED CONTROLLERS

##### A. Experimental Setup

Fig.8 illustrates "Torsional Vibration System Experimental Setup" specially made by Mitsubishi Heavy Industry based on our design. It consists of two brushless DC (BLDC) motors, changeable backlash and friction mechanism, the load equipment and so on. The generated torques of BLDC motors are controlled fast and precisely enough by two high performance motor drivers.

Sensor information from shaft encoders and tachogenerators are read into the microcomputer via the counter boards and A/D converters. After some control calculations, the torque commands are outputted to the motor drivers via D/A converters. Control algorithm is written by C language. We developed some more useful programs, e.g., frequency response measurement program using M-series test signal.

TABLE I gives the experimented control methods and their controller parameters. The inertia moments are given by the load-side (i.e. the torsional shaft side) quantities. We implemented

(1) original disturbance observer designed for 1-inertia system,

(2) fast resonance ratio control using fast disturbance observer,

and

(3) slow resonance ratio control proposed in this paper.

The speed controllers of (1) and (3) are designed for 1-inertia system, and in (2) we used Manabe Polynomial method.<sup>[8]</sup> In all experiments, I-P speed controllers are used by putting  $b=0$  in Fig.4.

In the experiments of the command response shown in Fig.9(a) ~ (c), the speed reference  $\omega_{ref}=10[\text{rad/s}]$  is given at  $t=0$ . In experiments of the disturbance response, at  $t=0$  the disturbance torque of  $2[\text{Nm}]$  is added from the loadside motor.

In the experiments here,  $\omega_{sL}$  is the load speed,  $\omega_{sg}$  the gear speed (We used the gear of 1/2 gear ratio.),  $\omega_m$  the motor speed and  $T_m$  the motor torque. We tried to set the gear backlash to be 0, but there still remains a small backlash. Also, note that the motor torque is limited by  $\pm 3.84[\text{Nm}]$ . In

the figures, the torque commands are drawn instead of the actual torques.

### *B. Experimental Results and Discussion*

The original disturbance observer in Fig.9(a) designed for 1-inertia system just suppresses the disturbance injected into the motor axis, which is the torsional torque in this case. As the result, big vibration was induced in the load speed and it considerably affected to the motor speed, too.

In the fast resonance ratio control shown in Fig.9(b), we implemented the disturbance observer whose estimation speed was designed as fast as possible. It was decided experimentally by control period, noise suppression characteristics, stability problem and so on.  $\omega_q (= 1/T_q) = 3.0\omega_a$  was the top speed of the disturbance observer. This is not fast enough to realize the ideal fast resonance ratio control aiming to  $K=3.025$ . We can see that the low frequency vibration can be suppressed effectively. However, the transfer function from  $T_L$  to  $\omega_L$  has a harmful frequency peak around 200[rad/s]. Due to this peak, relatively big high frequency vibration remains in the motor torque.

In the slow resonance ratio control, we chose  $K=2.368$ . In this case, the observer's speed is  $\omega_q = 1.7\omega_a$ , which is slower than that of the fast resonance ratio control. Although we recommended  $K=5 \sim 10$  in Chap. III, we did not need to use such a big  $K$  in the experimental system. This was because vibrational effect was partly suppressed due to the original friction in the actual system. Smaller  $K$  means slower disturbance observer. We took this advantage here. Fig.9(c) shows sufficiently stable time responses without any high frequency vibration in motor torque waveform, and frequency characteristics without any sharp peak. This is because there are no fast parts in the proposed controller.

## VI. CONCLUSION

In this paper, we proposed the "slow resonance ratio control" as an effective vibration suppression and disturbance rejection control method of torsional systems. We gave the explicit formula of the optimal estimation speed of the disturbance observer from the viewpoint of vibration suppression. We confirmed its superior performances by simulation and real experiment. In the original "fast resonance ratio control", we needed to design the speed controller considering the vibration suppression, where we dealt with the total system's characteristics given by higher order state equations. On the contrary, in the proposed slow resonance ratio control, we can use the speed controller independently designed for 1-inertia system. This has a great advantage in most industrial applications.

## REFERENCES

- [1] B. Wie and D. Bernstein, "A Benchmark Problem for Robust Control Design", *Proc. of ACC'90*, pp.961-962, 1990.
- [2] U. Schäfer and G. Brandenburg, "State Position Control for Elastic Pointing and Tracking Systems with Gear Play and Coulomb Friction -A Summary of Results-", *Proc. of 1991 EPE*, pp.2-596 ~ 2-602, Firenze, 1991.
- [3] Y. Hori, "Comparison of Vibration Suppression Control Strategies in 2-Mass Systems including a Novel Two-Degrees-Of-Freedom H<sub>∞</sub> Controller", *Proc. of 2nd International Workshop on AMC*, pp.409-416, Nagoya, 1992.
- [4] K. Yuki, T. Murakami and K. Ohnishi, "Vibration Control of a 2 Mass system by the Resonance Ratio Control", *Trans. of IEE-Japan*, Vol.113-D, No.10, 1993.
- [5] H. Umida, "Novel Control Strategies of Torsional Vibration System: A Dully Tuned Disturbance Observer", *IEEE-Japan IAS Annual Meeting*, S.12-3, 1994.
- [6] M. Iwata and S. Itoh, "High Performance and Adaptive Motion Control System Based on Identified Mechanical Parameter", *Proc. of 3rd International Workshop on AMC*, Berkeley, 1994.
- [7] S. Hara, et.al., "Benchmark Problem: Position Control/Velocity Control for Coupled Three-Mass System", *Proc. of ASCC'94*, pp.313-317, 1994.
- [8] S. Manabe, "Design of Velocity Controller for Three Inertia System by Coefficient Diagram Method", *Proc. of ASCC'94*, pp.329-332, 1994.
- [9] Y. Hori, "2-Mass System Control based on Resonance Ratio Control and Manabe Polynomials", *Proc. of ASCC'94*, pp.741-744, 1994.
- [10] Y. Hori, H. Iseki and K. Sugiura, "Basic Consideration of Vibration Suppression and Disturbance Rejection Control of Multi-Inertia System using SFLAC (State Feedback and Load Acceleration Control)", *IEEE Trans. on IA*, Vol.30, No.4, pp.889-896, 1994.
- [11] Y. Hori, "Comparison of Torsional Vibration Controls based on the Fast and Slow Disturbance Observers", *IPEC-Yokohama '95*, 1995.
- [12] Y. Hori, "Vibration Suppression and Disturbance Rejection Control on Torsional Systems", *Proc. of IFAC Workshop on Motion Control*, pp.41-50, München, 1995.
- [13] Y. Chun, et.al., "On Weighting Functions for H<sub>∞</sub> Controller and Its Experiment of 2-mass System with Low Frequency Resonance", *Proc. of IFAC Workshop on Motion Control*, München, 1995.
- [14] J.K. Ji and S.K. Sul, "Kalman Filter and LQ Based Speed Controller for Torsional Vibration Suppression in a 2-Mass Motor Drive System", *IEEE Trans. on IE*, Vol.42, No.6, pp.564-571, 1995.
- [15] K. Sugiura and Y. Hori, "Vibration Suppression in 2- and 3-Mass System Based on the Feedback of Imperfect Derivative of the Estimated Torsional Torque", *IEEE Trans. on IE*, Vol.43, No.1, pp.56-64, 1996.
- [16] Y. Hori, Y. Chun and H. Sawada, "Experimental Evaluation of Disturbance Observer-Based Vibration Suppression and Disturbance Rejection Control in Torsional System", *Proc. of PEMC'96*, Vol.1, pp.120-124, 1996.
- [17] Yoichi Hori, Hideyuki Sawada and Yeonghan Chun, "Slow Resonance Ratio Control for Torsional Vibration Suppression", *Proc. of ASCC'97*, Vol.1, pp.177-180, 1997.



## Captions of Figures and Tables

Fig.1. Typical configuration of steel rolling mill system.

Fig.2. 2-inertia system model.

Fig.3. Block diagram of 2-inertia system

Fig.4. Configuration of the slow resonance ratio control.

Fig.5. The peak amplitude at  $\omega_0$  v.s.  $K$ .

(When  $K$  increases, the peak at  $\omega_0$  decreases.)

Fig.6. The optimal estimation speed of the disturbance observer.

(For bigger  $K$ , faster estimation is needed.  $T_q = 1/\omega_q$ .)

Fig.7. Simulation results when  $K=5$ .

(a)  $R_0=J_L/J_{M0}=0.2$

(b)  $R_0=J_L/J_{M0}=1$

(c)  $R_0=J_L/J_{M0}=5$

Fig.8. Experimental setup of torsional vibration system.

(a) overview

(b) functions of components

Fig.9. Experimental results.

(a) Original disturbance observer

(b) Fast resonance ratio control

(c) Slow resonance ratio control.

TABLE I TESTED CONTROL METHODS AND PARAMETERS

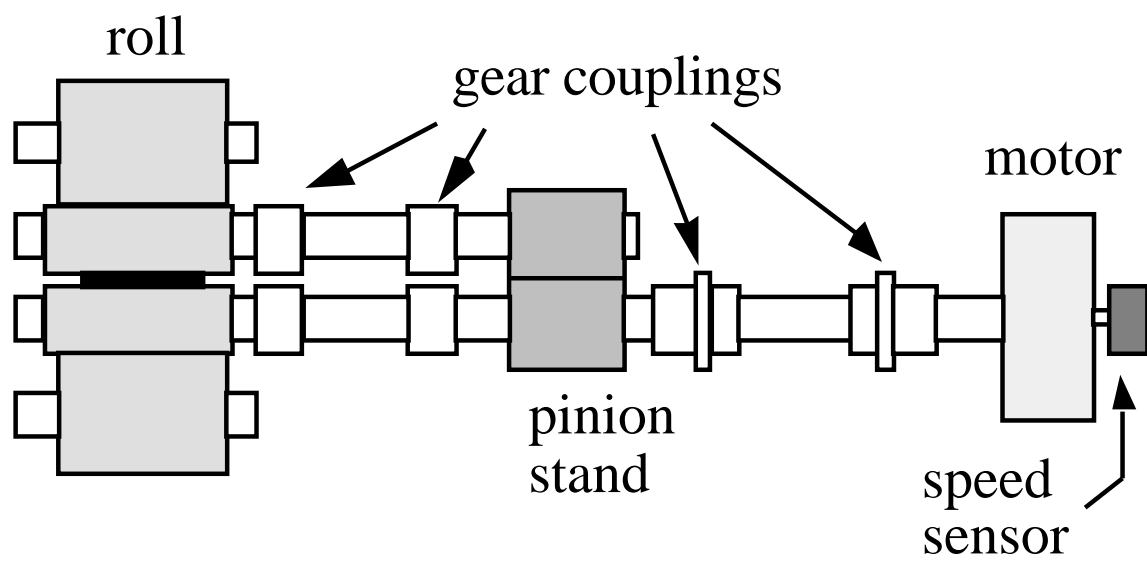


Fig.1. Typical configuration of steel rolling mill system.

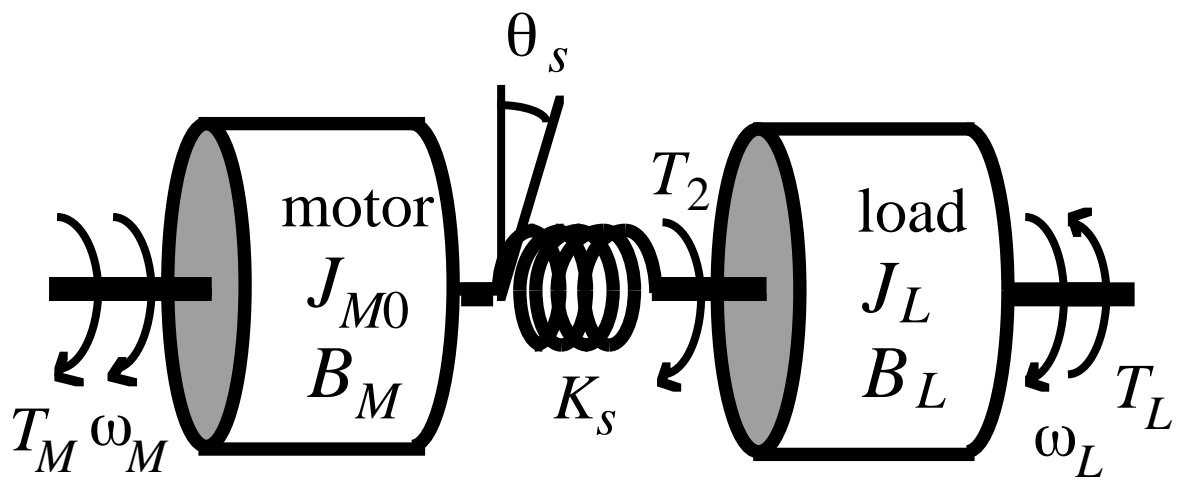


Fig.2. 2-inertia system model.

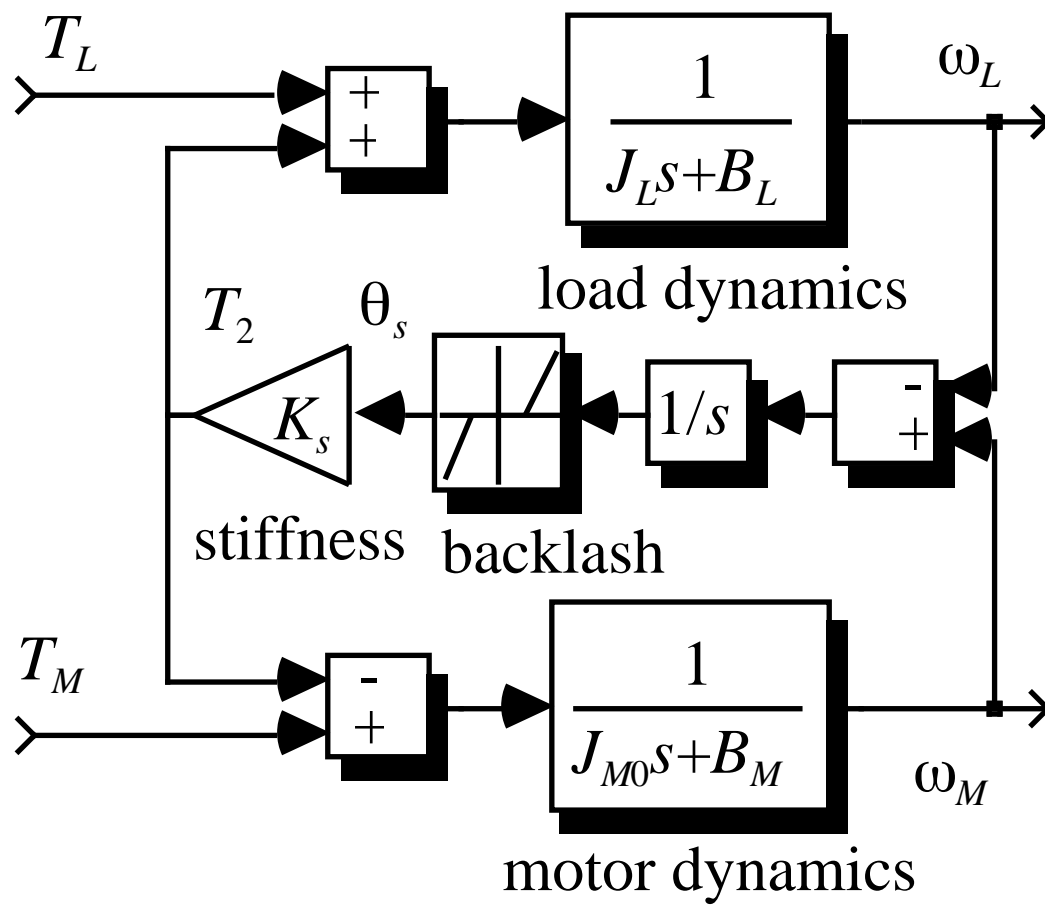


Fig.3. Block diagram of 2-inertia system.

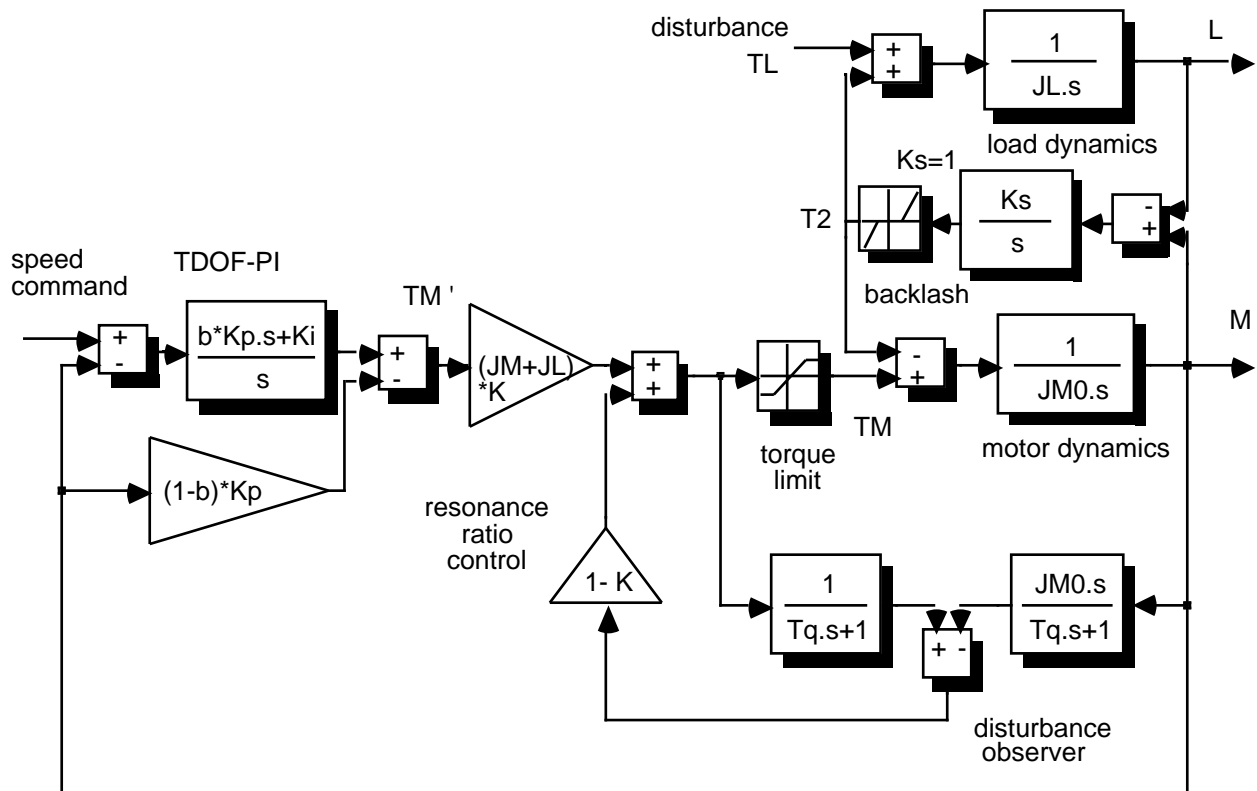


Fig.4. Configuration of the slow resonance ratio control.

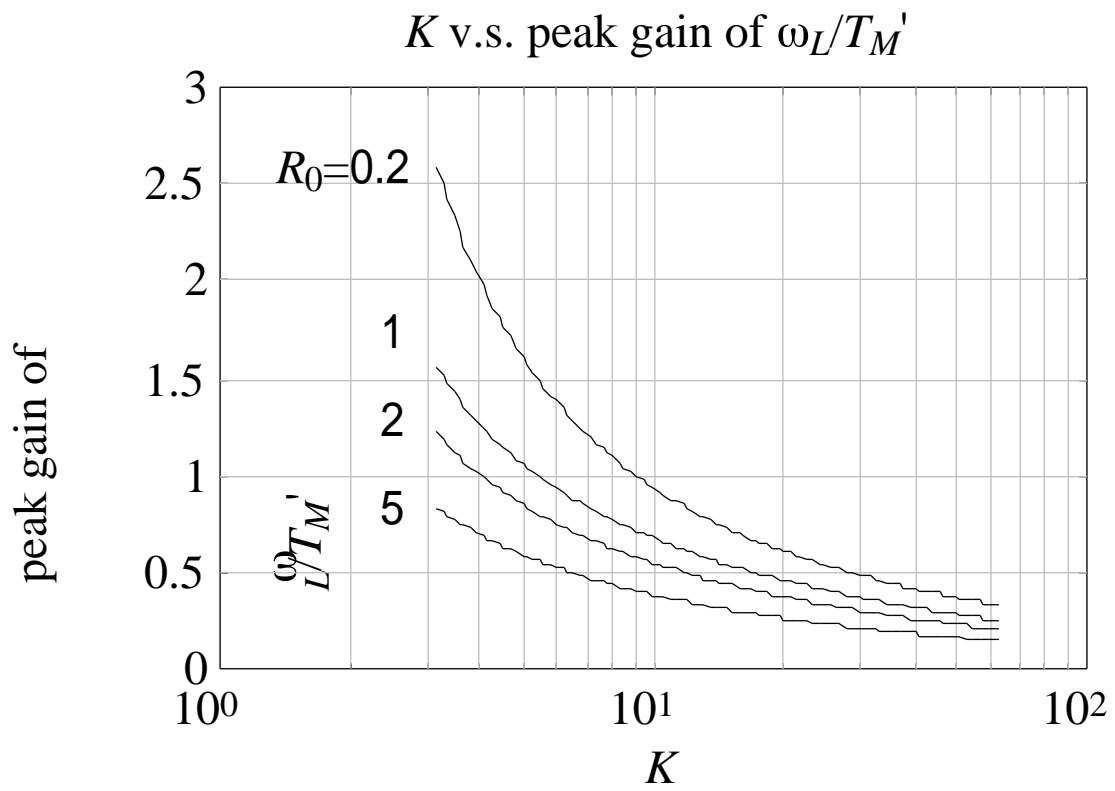


Fig.5. The peak amplitude at  $\omega_0$  v.s.  $K$ .  
(When  $K$  increases, the peak at  $\omega_0$  decreases.)

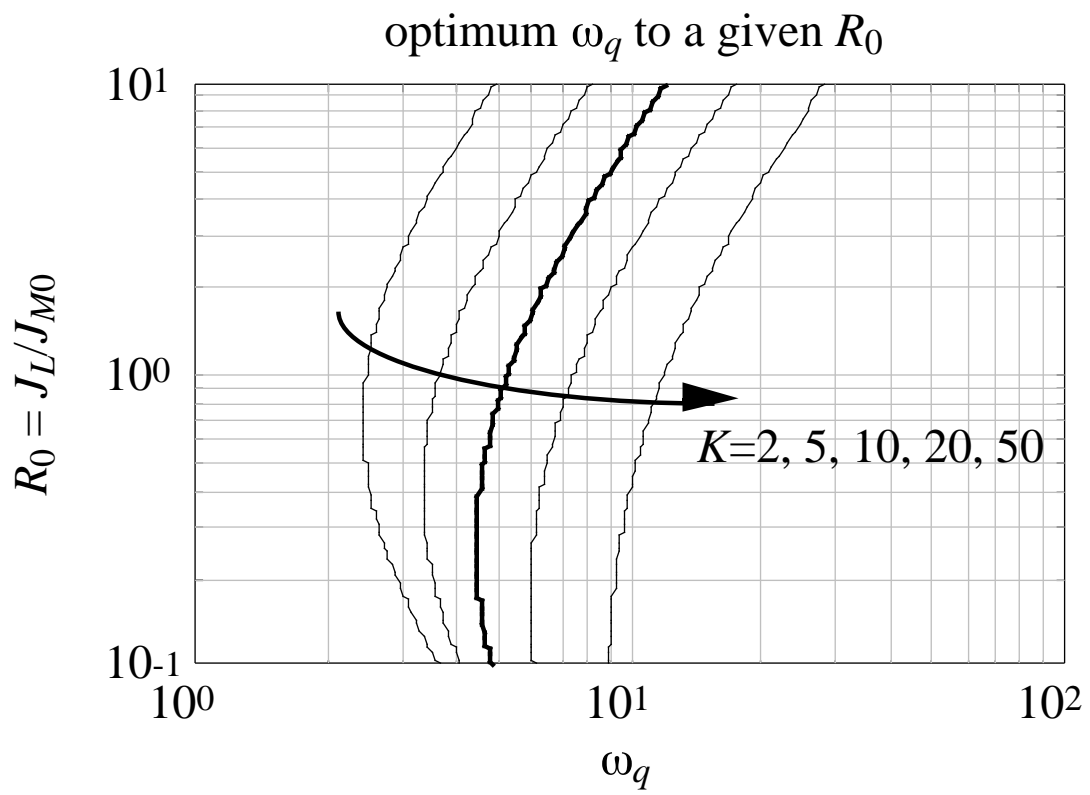


Fig.6. The optimal estimation speed of the disturbance observer.  
 (For bigger  $K$ , faster estimation is needed.  $T_q = 1/\omega_q$ .)

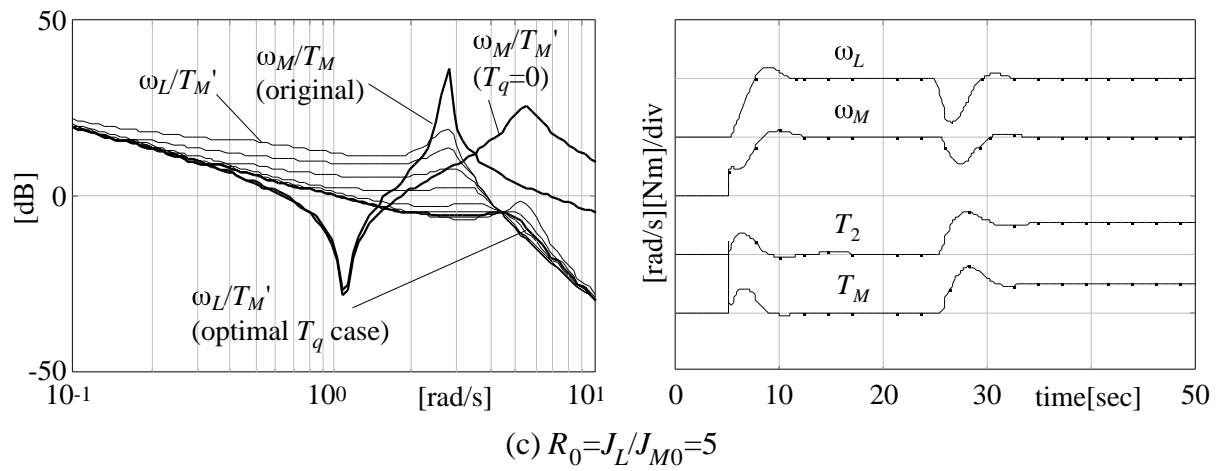
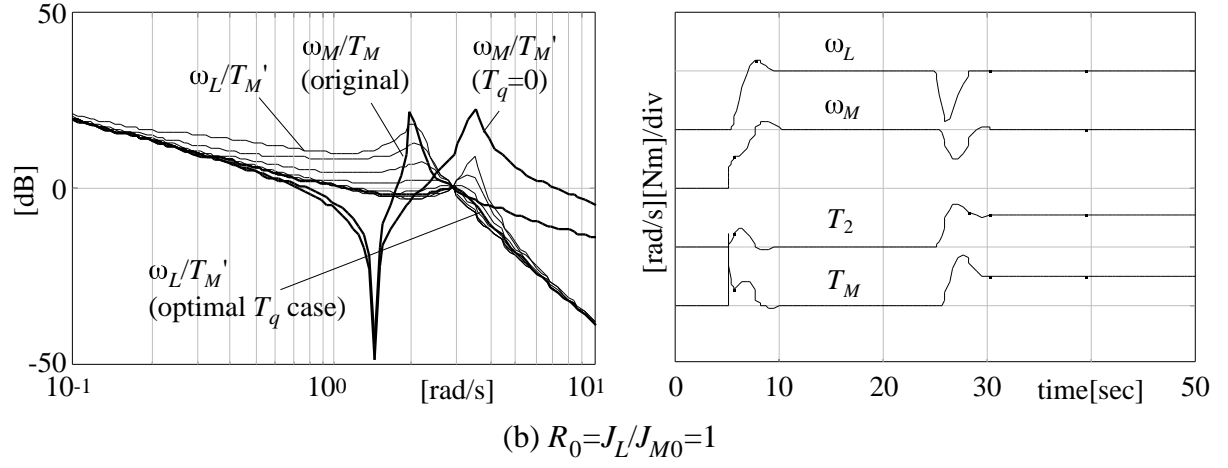
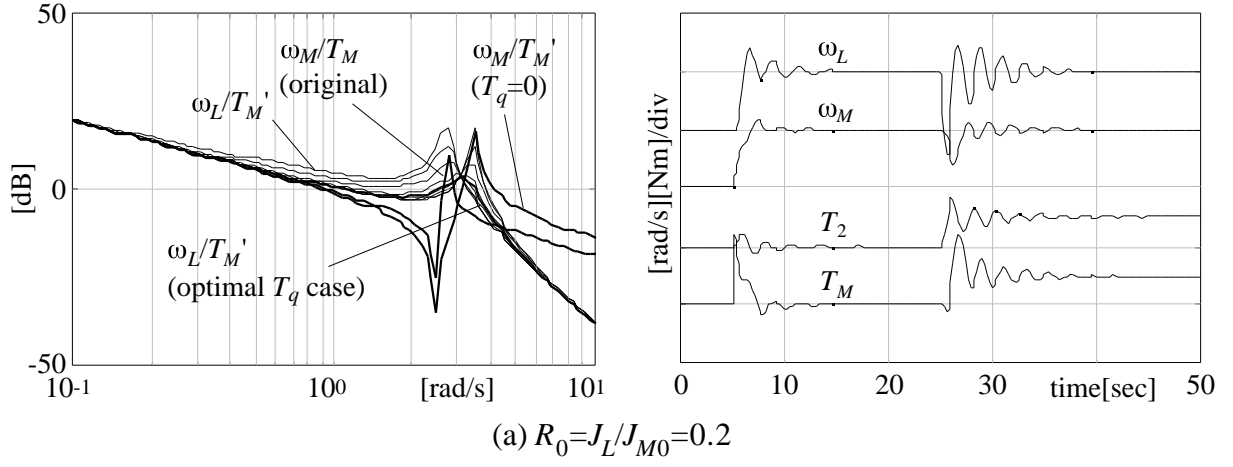
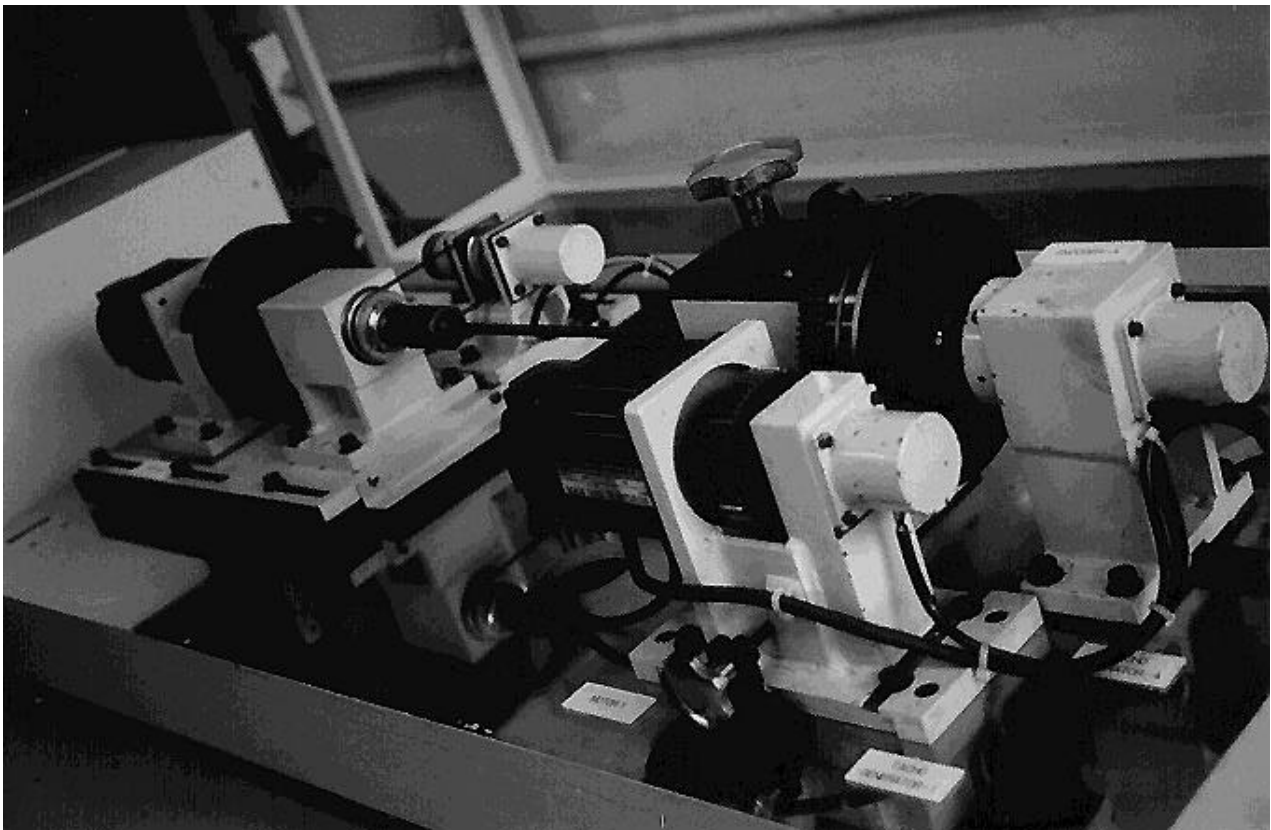
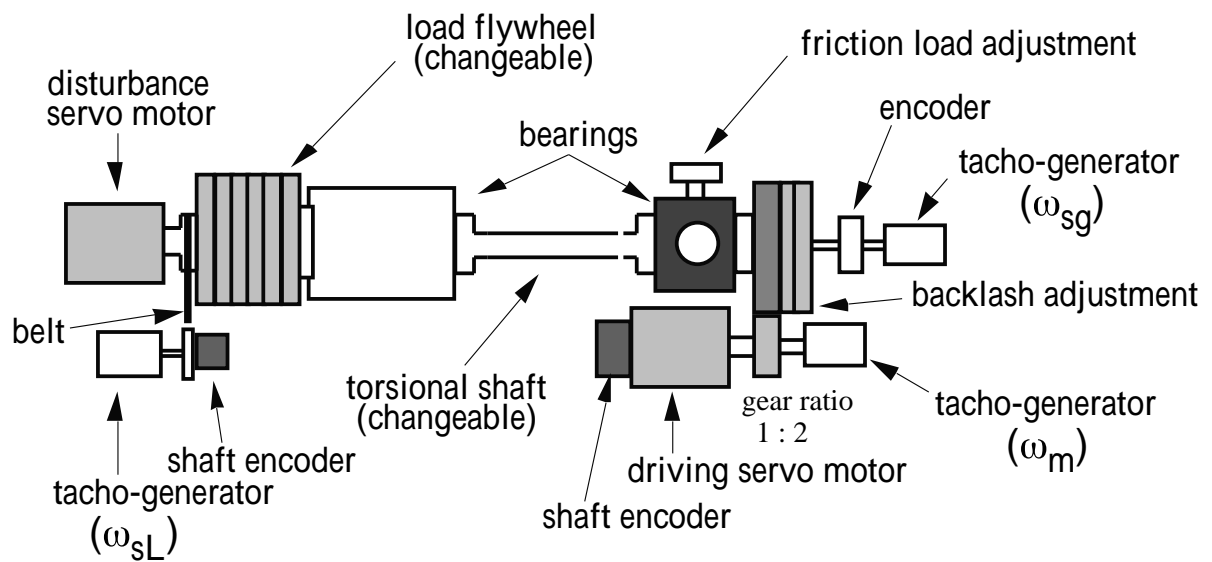


Fig.7. Simulation results when  $K=5$ .



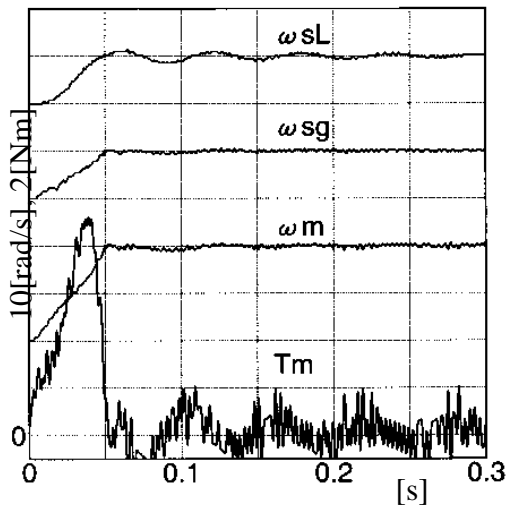


(a) overview

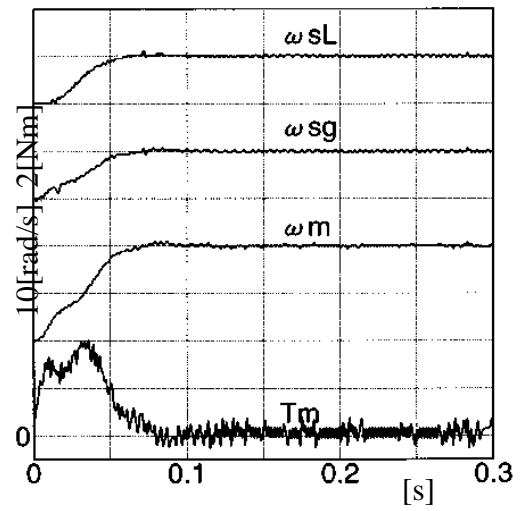


(b) functions of components

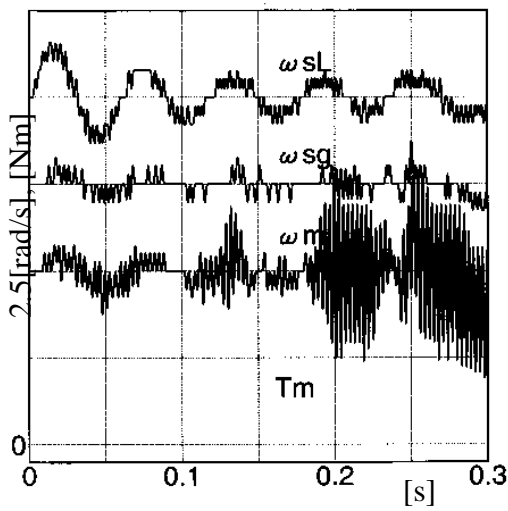
Fig.8. Experimental setup of torsional vibration system.



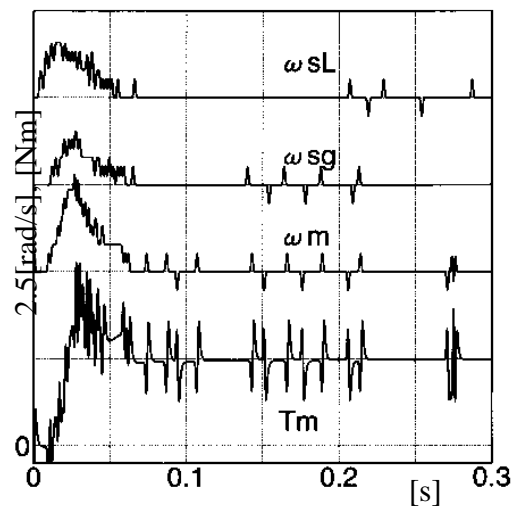
command response



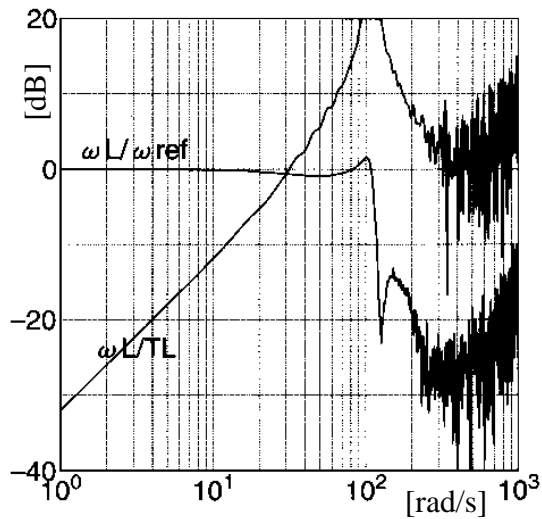
command response



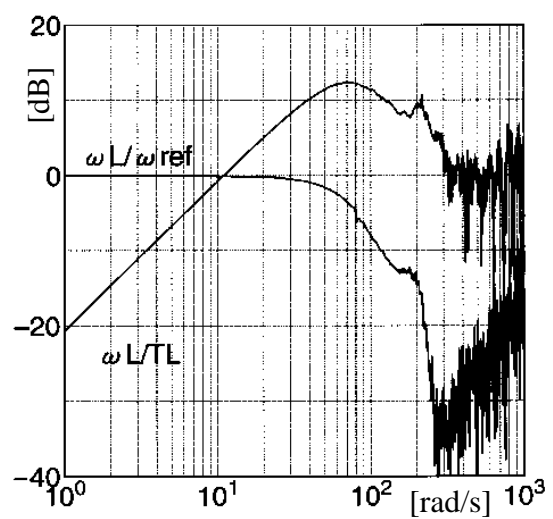
disturbance response



disturbance response



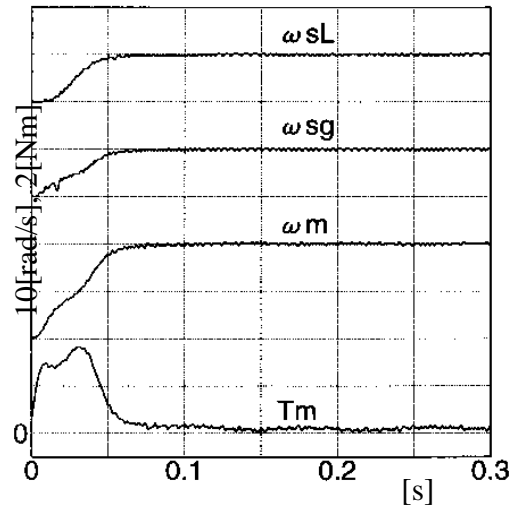
frequency response from  $\omega_{ref}$  and  $T_L$  to  $\omega_L$



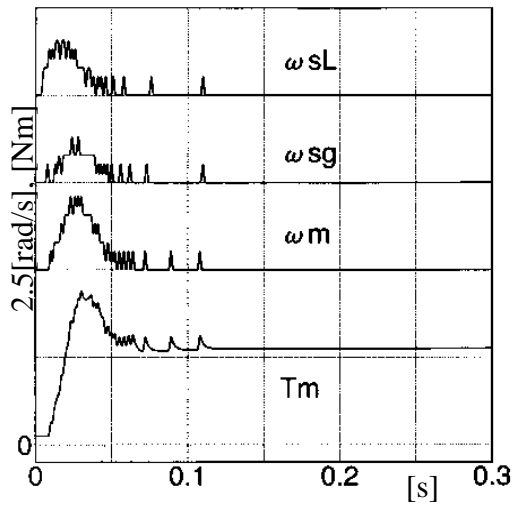
frequency response from  $\omega_{ref}$  and  $T_L$  to  $\omega_L$

(a) Original disturbance observer.

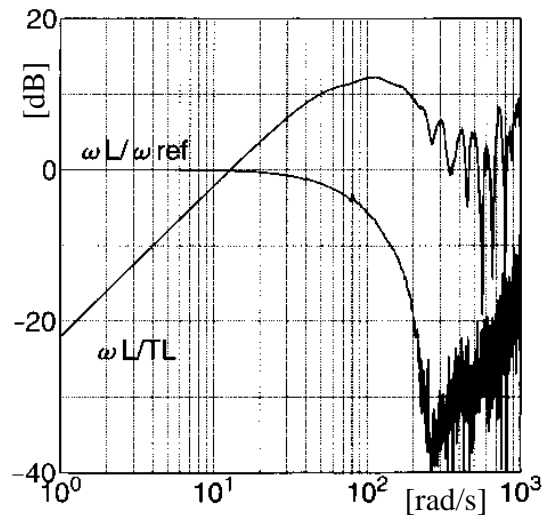
(b) Fast resonance ratio control.



command response



disturbance response



frequency response from  $\omega_{ref}$  and  $T_L$  to  $\omega_L$

(c) Slow resonance ratio control.

Fig.9. Experimental results.

TABLE I  
TESTED CONTROL METHODS AND PARAMETERS

<div>controller parameters</div>	disturbance observer for 1 axis	fast resonance ratio control	slow resonance ratio control
system parameters			
inertia moment of motor	$J_{M0}$ =4.016X10 <sup>-3</sup> [kgm <sup>2</sup> ]		
inertia moment of load	$J_L$ =2.921X10 <sup>-3</sup> [kgm <sup>2</sup> ]		
stiffness constant	$K_s$ =39.21 [Nm/rad]		
resonant frequency anti-resonant frequency	$\omega_{r0}$ =152.3[rad/s], $\omega_a$ =115.9[rad/s]		
inertia ratio resonance ratio	$R_0$ = $J_L/J_{M0}$ =0.7273, $H_0$ =1.314		
control period	$T_s$ =1[ms]		
parameters in speed control			
$K_p$ (proportional gain)	0.804	0.435	0.535
$K_i$ (integral gain)	26.6	14.26	17.71
parameters in vibration control			
$K$ ( = $R/R_0$ )	--	3.025	2.368
$\omega_q$ ( = $1/T_q$ ) *	$2.0\omega_a$	$3.0\omega_a$	$1.7\omega_a$

\*  $T_q$  : time constant of the disturbance observer